SIZE-CONTROLLED SYNTHESIS OF CARBON NANODOTS

A Thesis

Presented to the Faculty of the Graduate School

of Cornell University

In Partial Fulfillment of the Requirements for the Degree of

Master of Science

by

Yubo Zhai

August 2016

ABSTRACT

This paper reports a robust method to synthesize size-controlled fluorescent carbon nanodots by crosslinking with hexamethylene diisocyanate. First, 5nm C-dots are synthesized. Hexamethylene Diisocyanate (HDI), the crosslinker, is then added. It reacts with terminal groups (-OH) on the surface of the C-dots forming urethane bonds, which crosslink and agglomerate C-dots. A series of experiments varying the molar ratio of hexamethylene diisocyanate to C-dots showed that the size of the crosslinked C-dots depends on the molar ratio. Crosslinked C-dots also share the same fluorescent property with the small size C-dots.

BIOGRAPHICAL SKETCH

Yubo was born in Henan province, China and received his B.S. degree in Applied Chemistry from Shanghai Jiao Tong University. He is currently a master student in department of Material Science and Engineering under the supervision of Professor Archer. His main research interest is carbon nanoparticles.

ACKNOWLEDGMENTS

I would like to give my deepest appreciation to Professor Archer, Professor Cathles and Professor Hurwitz for their guidance in my research. I would also like to thank Snehashis, Russell, Caryl and Adam for their help throughout this research. Thanks all the people in Archer research group for being a family.

TABLE OF CONTENTS

INTRODUCTION

Fluorescent particles have been applied in electronic materials, light emitting diodes and many other devices used in our daily lives. Nanoscale fluorescent particles can also be used as efficient tracers, because they do not diffuse away from the fractures or channels where flow occurs and their concentration can be determined by their fluorescence. [1]

Nowadays, the most widely used fluorescent particles are quantum dots. Quantum dots are known as small size single crystals whose fluorescent property can be influenced by their composition and synthetic condition. Quantum dots usually have size-dependent absorption and emission. [2] However, quantum dots are based on metallic elements which raise concerns over the toxicity. Carbon nanodots (C-dots) have attracted intensive attention in recent years as replacements for metal-based quantum dots because of their strong fluorescence, high aqueous solubility, easy functionalization, low toxicity and good biocompatibility properties.[3-7] Carbon nanodots were first obtained during purification of carbon nanotubes in 2004.[8] When processing a suspension of single-walled carbon nanotubes by gel electrophoresis, researchers found that the suspension could be separated into three distinct classes of nanomaterials, including a highly luminescent material.

Today, different methods to synthesize C-dots have been reported.[9-12] Basically, the two main synthetic methods can be described as top-down and bottom-up methods. In the top-down approach,[13-19] C-dots are obtained from larger carbon structures like graphite powders. Small particles can be produced by arc discharge[8,17] and laser ablation.[13] A one step synthesis method was introduced by Hu et al.[13] In this method, a

laser with wavelength of 1.064 μm was used to stimulate graphite powders, which were dispersed in poly (ethylene glycol) (PEG200N) with the energy density of 6.0×10^6 W cm^2. Ultrasound was also applied to accelerate the movement of carbon particles. After 2 hours, the C-dots were collected and analyzed. These C-dots' average size was about 3nm. Another experiment used water as the solvent instead of poly (ethylene glycol) (PEG200N). The particles prepared in water were then oxidized and analyzed. These two experiments showed that the surface state is responsible for the photoluminescence of carbon nanoparticles. [9,16]

In the bottom-up approach, [20-26] C-dots are formed by molecular reactions. Typically, this method includes thermal and microwave treatment.[21] Krysmann et al.[15] controlled the particles size and fluorescence by adjusting the pyrolysis temperature of citric acid and ethanolamine. No particles were detected after pyrolysis at 180℃. Pyrolysis at 230℃ produced carbon nanodots with size around 18nm. Higher pyrolysis temperatures produced smaller particles until the particles aggregated at 400℃. They analyzed the particles and concluded that during pyrolysis the precursor molecules were carbonized to form carbon cores, and the strong PL (photo luminescent) property of the particles was due to the formation of amide bonds. However, efficient methods to synthesize size-controlled C-dots are still a challenge in this field. Here, we report a robust method to synthesize size-controlled carbon nanodots by crosslinking with hexamethylene diisocyanate.[25-32] In this reaction, hexamethylene diisocyanate forms strong urethane bonds with hydroxyl groups on the surface of small previously synthesized C-dots, crosslinking these C-dot particles to produce larger particles. A series of experiments varying the ratio of hexamethylene

diisocyanate to precursor C-dots showed that the C-dots' size increase with ratio of hexamethylene diisocyanate to precursor C-dots. Crosslinked C-dots also share the same fluorescent property with the small size C-dots. Following this rule, different sizes of C-dots can be produced.

EXPERIMENTAL SECTION

Materials. Citric acid, ethanolamine and hexamethylene diisocyanate were purchased from Sigma-Aldrich. All reagents were of analytical grades and used without further purification.

Preparation of precursor C-dots. Our precursor C-dots were synthesized using the method reported by Li et al.,[2] a one-step thermal pyrolysis of citric acid and ethanolamine at 200℃ for 8h with 1:3 molar ratio. C-dots were prepared as follows: citric acid (9.6g) was dissolved in DI-water (10 mL) and then ethanolamine (9.15g) was added. After 30 minutes, the solution (named as precursor) was transferred into an oven and heated at 200℃ for 8h (as shown in Scheme 1). After the reaction, the sample was cooled to room temperature naturally. The product, which was brown-black solid, was collected and properly stored. These C-dots were named "precursor C-dots".

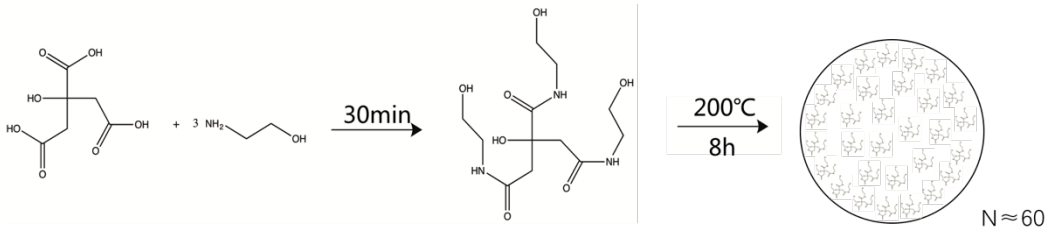

Scheme 1. Synthetic route of precursor C-dots.

Preparation of Crosslinked C-dots. 0.24g precursor C-dots was dissolved in 2ml DMF and then different amounts of hexamethylene diisocyanate were added, with constant stirring at 200 rpm. After 24h the crosslinked C-dots were collected from the solution and stored (as shown in Scheme 2).

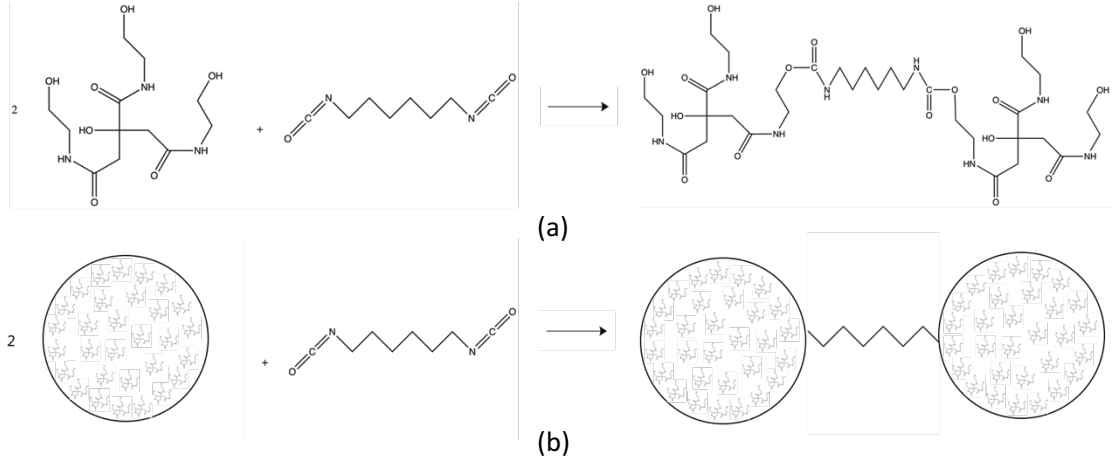

Scheme 2. Illustration of the formation process of crosslinked C-dots.

Scheme 2 shows the synthetic route for crosslinked C-dots. HDI acts as the linkage between the precursor C-dots and eventually form crosslinked C-dots. Fig 2a shows the reaction on the surface of two precursor C-dots. Fig 2b illustrates how the crosslinking of two precursor C-dots could be achieved by an HDI molecule.

Instrumentation. Transmission Electron Microscopy (TEM) measurements were made with a FEI T12 Spirit. Photoluminescence spectra were performed using **S**pectraMax M2e Multi-Mode Microplate Reader (aqueous dispersions of samples were measured in disposable plastic cuvettes). FT-IR spectra of the samples were carried out by a Thermo Scientific Nicolet iZ10 FT-IR spectrometer.

RESULTS AND DISCUSSION

The FTIR spectra, transmission electron microscope (TEM) images and size distribution of the precursor C-dots are shown in Fig 1.

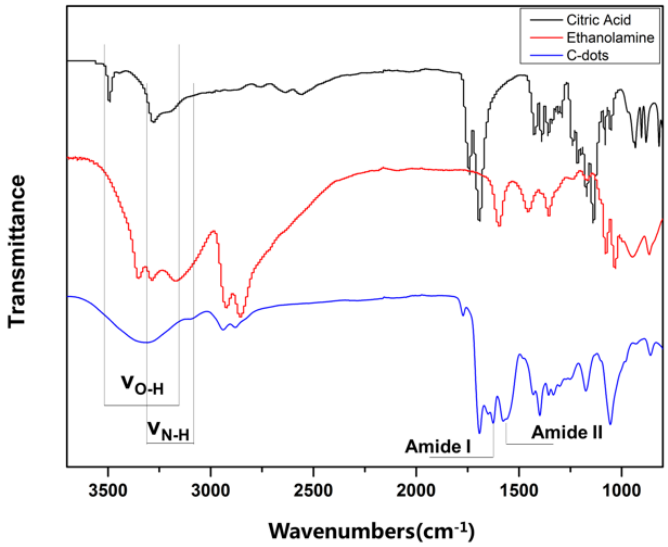

(a)

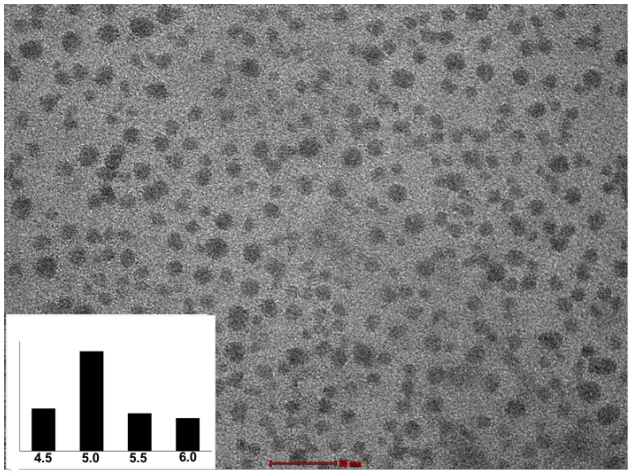

(b)

Figure 1. (a) Fourier transform infrared spectra of citric acid, ethanolamine and precursor C-dots. (b) TEM image and size distribution of the precursor C-dots (scale bar is 50nm).

The FTIR spectra of C-dots confirms the presence of amide bonds, as evidenced by their vibrational fingerprints centered at 1639 cm^{-1} (C=O stretching of the amide bond), and 3300 cm^{-1} (N−H stretching). The broad peak around 3300cm^{-1} confirms the existence of O-H functional groups. Peaks that correspond to different functional groups are noted and identified in Figure 1a. The spectrograph confirms the condensation reaction between citric acid and ethanolamine.[5,15] Figure 1b shows the size and shape of precursor C-dots. The precursor C-dots are nearly spherical with a narrow size distribution around 5nm. The small size and spherical shape is consistent with other researcher's work. [19,21]

m_1(g) M_{flask}	m_2(g) $M_{flask+c\text{-}dots}$	m_3(g) $M_{flask+c\text{-}dots+toluene}$	m_2-m_1(g) $M_{C\text{-}dots}$	m_3-m_2(g) $M_{solvent}$	$M_{solvent}$/0.867 $V_{solvent}$(ml)	50-$V_{solvent}$ V_{cdots}(ml)	ρ(g/ml) $M_{C\text{-}dots}/V_{C\text{-}dots}$
42.66	43.01	85.81	0.35	42.80	49.37	0.63	0.54
36.25	36.49	79.40	0.24	42.91	49.49	0.51	0.46
42.66	42.84	85.82	0.18	42.98	49.57	0.43	0.43
36.25	36.45	79.43	0.20	42.98	49.58	0.42	0.48
10.26	10.45	18.78	0.19	8.33	9.61	0.39	0.49
10.26	10.40	18.81	0.14	8.41	9.70	0.30	0.46
							0.48

Figure 2. Density measurement of precursor C-dots (in toluene).

C-dots are insoluble in toluene which makes it an ideal solvent to measure the density of precursor C-dots. We used 50ml and 10ml volumetric flask with different amounts of precursor C-dots. We measure the mass of flask m_1, mass of flask with C-dots m_2 and the mass of flask with C-dots and solvent m_3. In this way, m_2-m_1 is the mass of precursor C-dots and m_3-m_2 is the mass of solvent. Since we know the density of toluene is 0.867 g/ml, we can calculate the volume of toluene. From the volume of

volumetric flasks (50ml or 10ml), we can determine the volume of the C-dots. Dividing the mass by the volume of C-dots, we determine that the density is 0.48 g/cm^3 (compared with a carbon density of 2.25g/ cm^3). The average size of precursor C-dots of 5nm together with the precursor C-dots density of 0.48 g/cm^3, indicates the molecular weight of precursor C-dots is 1.87*10^4 g/mol. Since the molar mass of precursor molecules is 321 g/mol (192+61*3-54), approximately 60 precursor molecules are aggregated into each precursor C-dot during the carbonization process shown in scheme 1.

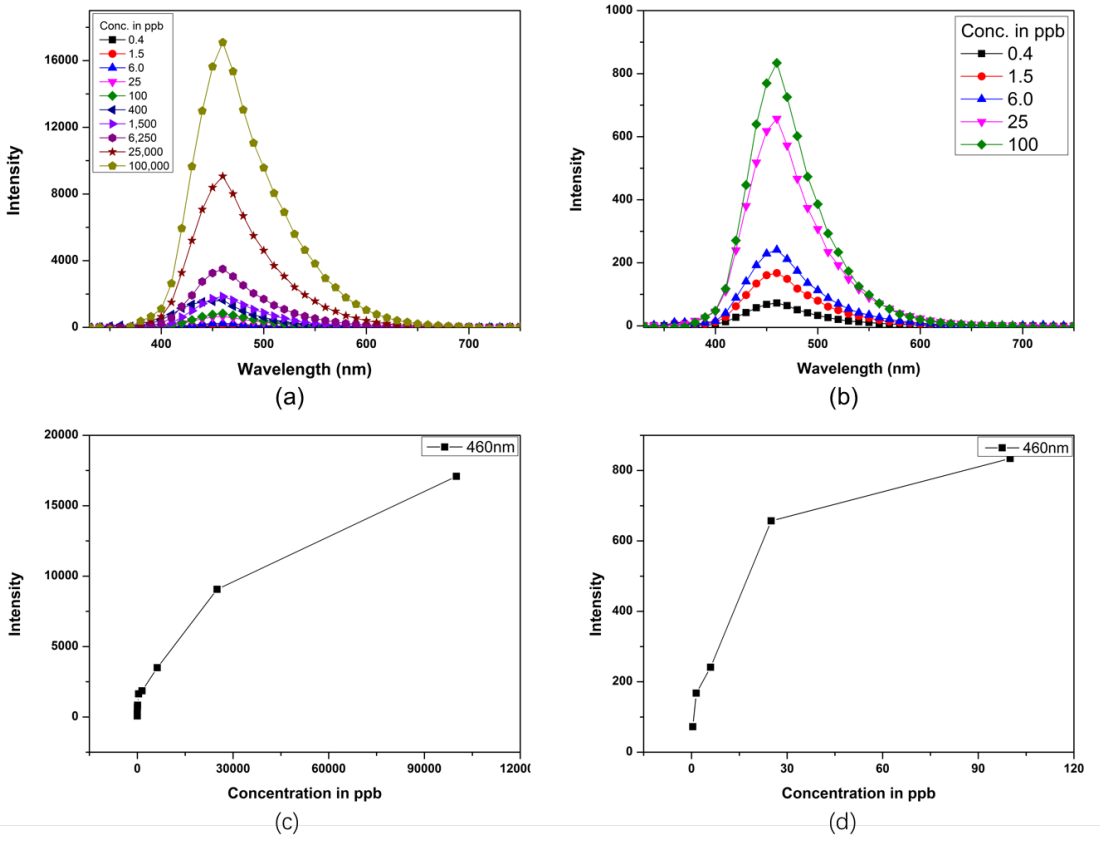

Figure 3. PL spectra of aqueous dispersions of precursor C-dots: (a) Concentration ranging from 0.4ppb to 100,000ppb. (b) Concentration ranging from 0.4ppb to 100ppb. The peak fluorescence emission at 460nm: (c) Concentration ranging from 0.4ppb to 100,000ppb. (d) Concentration ranging from 0.4ppb to 100ppb.

Figure 3 shows that the PL spectra of the C-dots, with wavelength ranging from 350 nm to 750 nm, has strong dependence on concentration. The peak fluorescence emission intensity is obtained at 460nm. The spectra show the PL property of different concentrations, from 0.4ppb to 100,000ppb (parts per billion). With the increasing of concentration from 0.4ppb to 100ppm, the overall fluorescence intensity also increases accordingly. We can tell from the spectra that different concentrations share the same shape and the C-dots are still detectable even down to 0.4 ppb. These results suggest that CDs may be used as a powerful tracer in biology applications or diagnosing subsurface fluid flow pathways. The PL spectra is similar to the result reported by Yang[10], Hu[12], Krysmann[15] and Ming[16]. In all cases there were strong PL peaks in the excitation wavelength range from 300nm to 800nm. Krysmann used the same synthesis chemistry as we do and concluded that amide groups in the precursor molecules were responsible for the photoluminescence. Yang and Ming had a different decoration chemistry that did not include amides, but their carbon particles nevertheless showed strong photoluminescence.

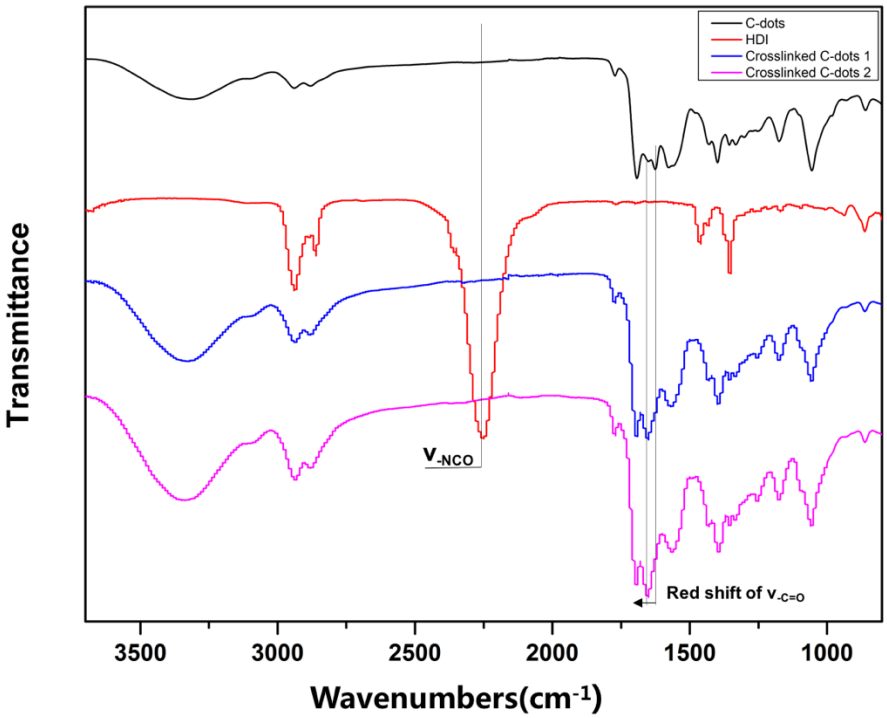

Figure 4. Fourier transform infrared spectra of precursor C-dots, HDI and two different batches of crosslinked C-dots.

Figure 4 shows the FTIR spectra of precursor C-dots, HDI and two different batches of crosslinked C-dots. Peaks that correspond to functional groups are noted and identified. The reaction process is confirmed by the disappearance of the 2275cm^{-1} peak (–NCO group of HDI) and the red shift of the –C=O peak, which is an indication of the existence of oxygen atom next to the –C=O bond. The disappearance of –NCO peak also indicates all the HDI has been fully consumed in the reaction.

Since there are approximately 60 precursor molecules in one precursor C-dot particle, as we can see from the Scheme 1, one C-dots particle has more than one reaction sites for HDI molecules. This indicates the number of HDI molecules attached on every precursor C-dots is controlled by the mount of HDI we added. Once a precursor C-dot acts as a nucleus, the number of C-dot particles attached on this nucleus is proportion to the amount of HDI. More C-dots agglomerated together increases the size of the crosslinked C-dots.

Serial Number	C-dots mol / 10^{-5}	HDI mol / 10^{-5}	Ratio HDI/C-dots	Size /nm
1	1.28	30	23.4	378
2	1.28	24	18.75	190
3	1.28	5.4	4.22	152
4	1.28	4.2	3.28	95
5	1.28	2.4	1.88	85
6	1.28	2.2	1.72	81
7	1.28	2.0	1.64	74
8	1.28	1.8	1.41	61
9	1.28	1.5	1.17	56
10	1.28	1.2	0.94	47
11	1.28	0.6	0.46	42
12	1.28	0.06	0.05	14

Table 1. Experiment series. All the experimental condition remains the same except for the amount of HDI.

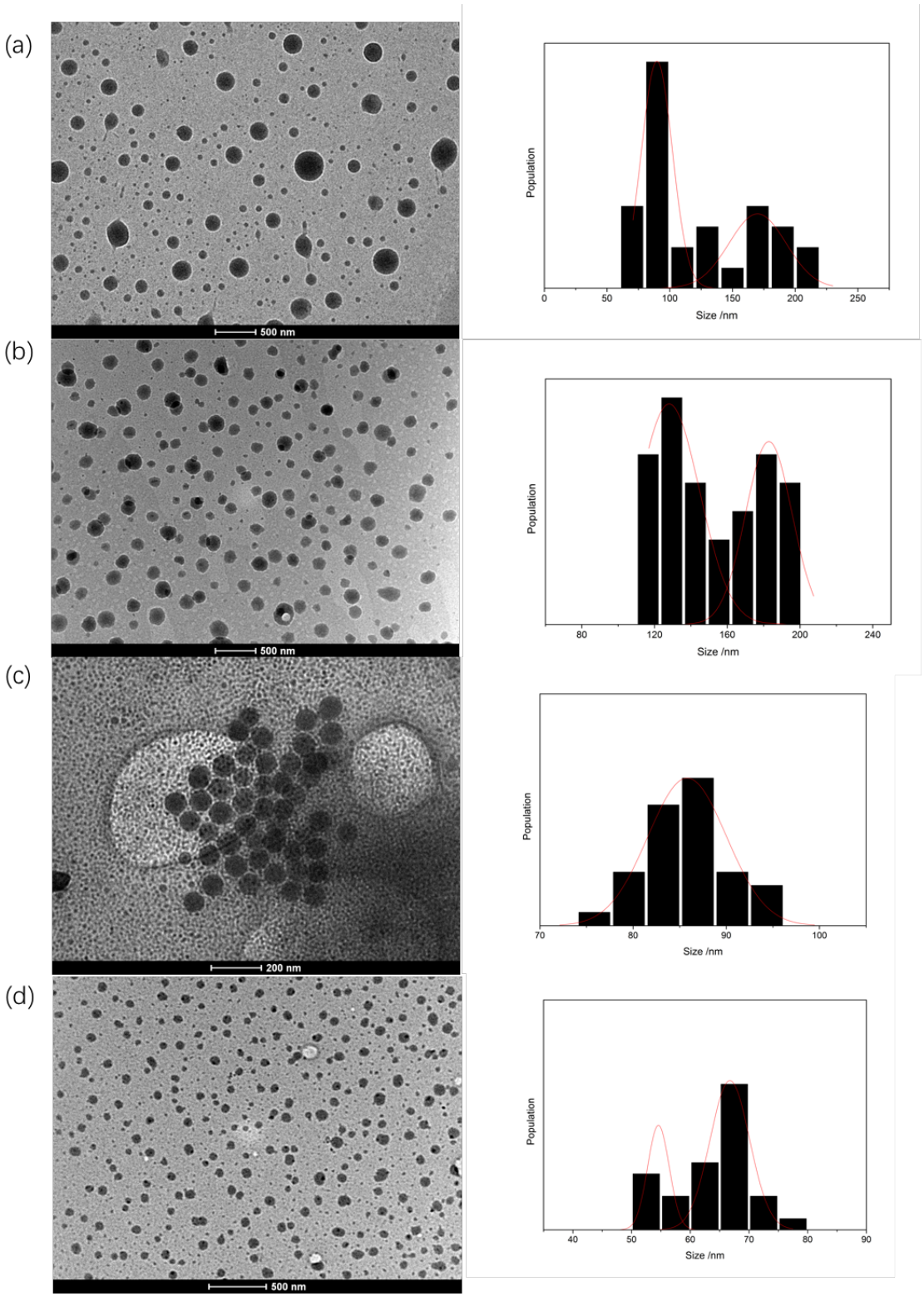

Figure 5. TEM images and size distributions of crosslinked C-dots synthesized by experiment series (a) #2 (b) #3 (c) #5 (d) #8.

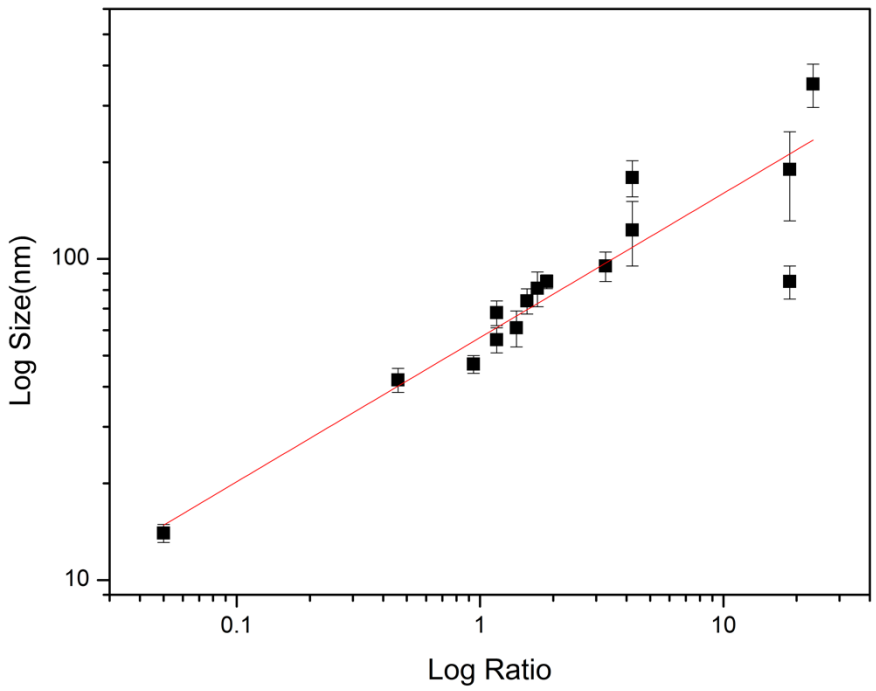

Figure 6. Average particle size and geometric standard deviation for experiment series shown in Table 1. HDI/precursor C-dot molar ratio changes from 0.05 to 23.4. Multiple points at same molar ratio indicates the spreads in bimodal size distributions.

Fixing all experimental conditions (room temperature, 2ml DMF, 200rpm stirring rate, 24h reaction time) except the amount of HDI, shows the relationship between size and molar ratio. As we can see from the transmission electron microscopy (TEM) images shown in Figure 5, crosslinked C-dots show near spherical morphology, which is similar to precursor C-dots. Some of their size distributions are bimodal and the standard deviation becomes larger with the increasing [HDI]. This could be for two reasons: First, higher [HDI] means more reaction sites on the surface of C-dots. Thus the higher [HDI] makes it easier for the C-dots to build linkages and this will make the

distribution more dispersed. Second, when the ratio of [HDI] to [C-dots] is low, the reaction of isocyanate is mainly with –OH functional groups. Reaction of isocyanate with –NH functional groups starts to happen when the ratio of [HDI] to [C-dots] is increased, and this promotes C-dot crosslinking and dispersity. When we plot the log of the size of the cross-linked C-dots (Y axis) against the log of the molar ratio of [HDI] to [precursor C-dots] (X axis), we find $size = \sqrt{[HDI]/[\text{precursor C} - \text{dots}]}$.

Several factors that may influence the crosslinking process. First, reactants concentration: Our experiments are carried out with $1.28*10^{-5}$ mol precursor C-dots in 2ml DMF with different amount of HDI. Higher concentration increases the number of collisions per unit time and makes it easier to form linkages between pairs of precursor C-dots. Compared with our result, experiments with higher concentration may have larger size and larger dispersity. Second, temperature: Higher temperature means faster particles movement and higher energy, which creates more collisions between C-dots particles per unit time thus can form linkage quicker. On the one hand, this may shorten our reaction time. On the other hand, this may lead to more dispersed crosslinked particles. If we executed a series of experiments under higher temperature conditions, experiments with high [HDI] may have multimodal size distribution and larger standard deviation, and the slope of the line in Figure 6 should become larger. The stirring rate may have the same effect as temperature. If we want to get more monodispersed crosslinked C-dots, reducing the reaction temperature (stirring rate) may be an efficient way. Third, time: Shorter time means the total number of collisions are smaller which means the degree of crosslinking is smaller. Therefore, if we collect the sample at 6h, 12h, 18h, 24h and compared their sizes, the size and

dispersity should become larger with the increasing of time. In a word, if we want to get monodispersed, relatively smaller size crosslinked C-dots, low concentration, low temperature (stirring rate)and shorter reaction time may be the best way.

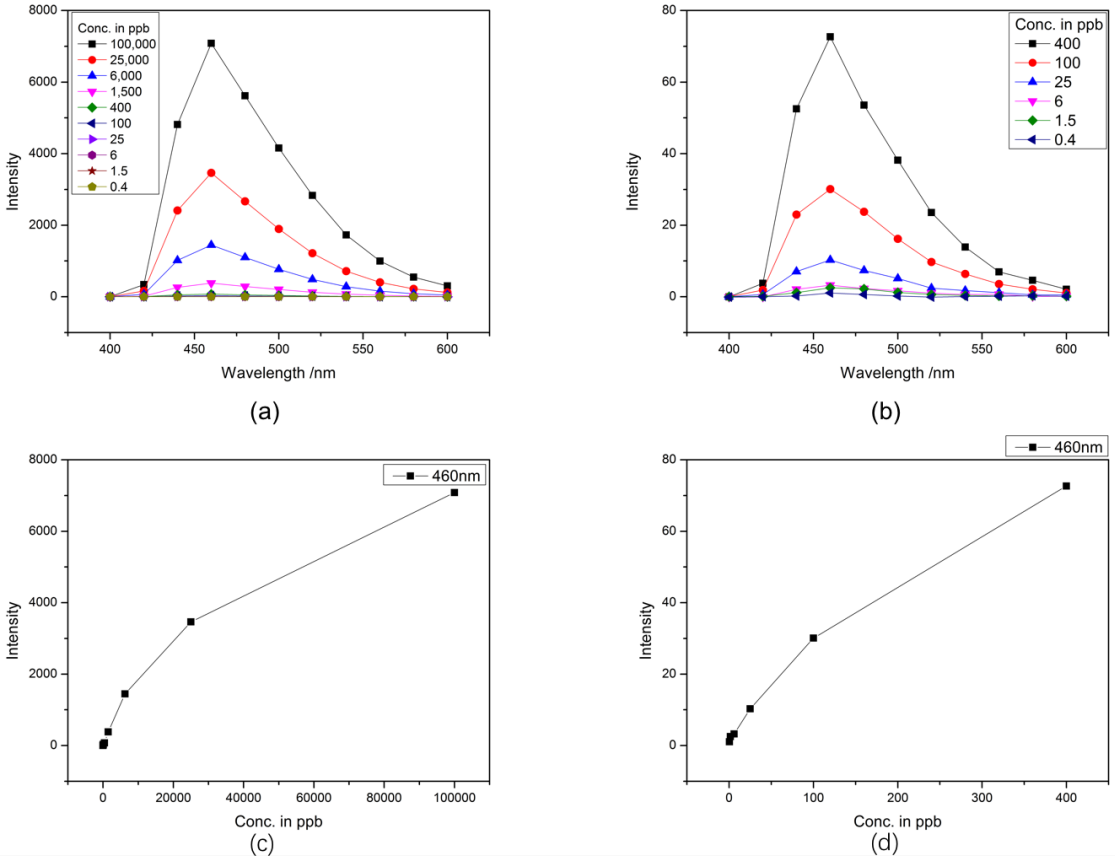

Figure 7. PL spectra of aqueous dispersions of crosslinked C-dots synthesized by Serial Number 7: (a) Concentration ranging from 0.4ppb to 100,000ppb, (b) Concentration ranging from 0.4ppb to 400ppb. Maximum fluorescence emission intensity spectra at 460nm: (c) Concentration ranging from 0.4ppb to 100,000ppb, (d) Concentration ranging from 0.4ppb to 400ppb.

When the excitation wavelength is 358nm, C-dots show the maximum emission intensity at 460nm. Crosslinked C-dots share the same property with precursor C-dots as shown in Figure 7 and Figure 8. We extract the different size crosslinked C-dots' PL intensity at 460nm (100ppm, 25ppm and 6ppm) and list the result in table 2. When we plot the log of the particle size (X axis) against log of peak PL (Y axis) the plot

shows PL$\propto 1/(\text{size})^2$. Krysmann[15] reported that fluorescence of C-dots made by citric acid and ethanolamine comes from the amide groups. These functional groups on the surface are also the source of fluorescence for crosslinked C-dots. The relationship between intensity and size is influenced by two factors. One is the surface area of crosslinked C-dot and the other one is the blockage by other crosslinked C-dots.

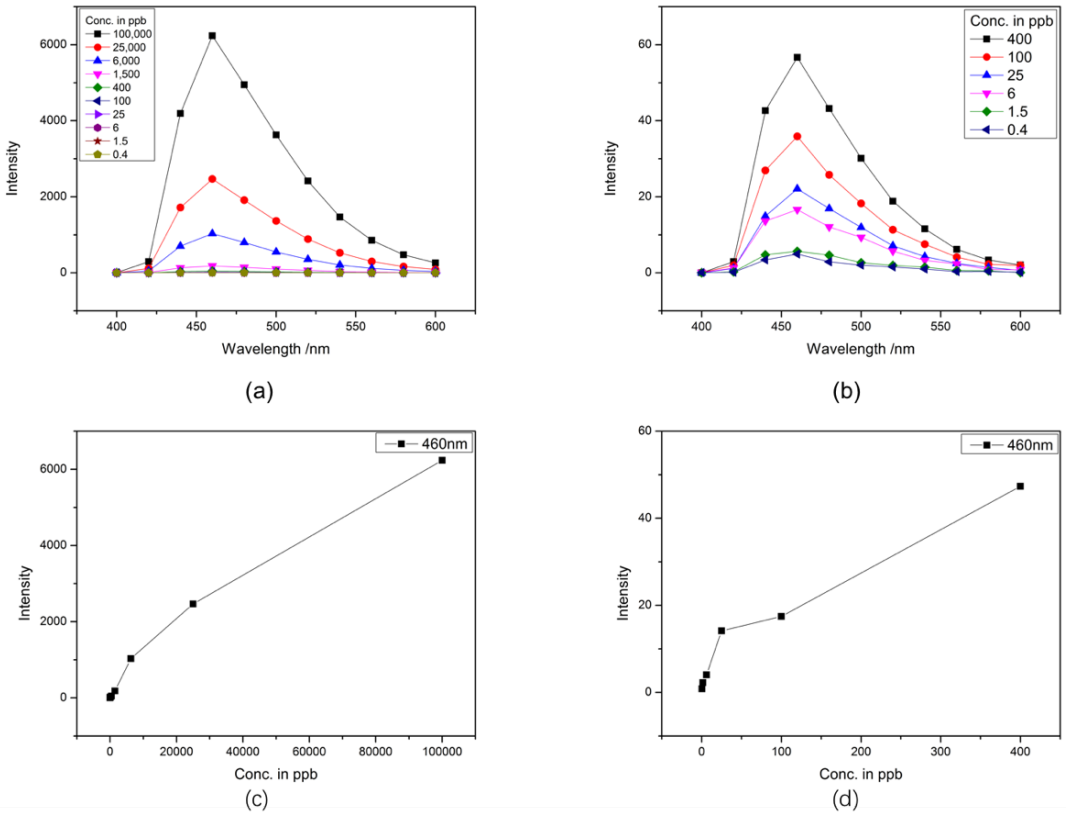

Figure 8. PL spectra of aqueous dispersions of crosslinked C-dots synthesized by Serial Number 10: (a) Concentration ranging from 0.4ppb to 100,000ppb, (b) Concentration ranging from 0.4ppb to 400ppb. Maximum fluorescence emission intensity spectra at 460nm: (c) Concentration ranging from 0.4ppb to 100,000ppb, (d) Concentration ranging from 0.4ppb to 400ppb.

Serial Number	Size/nm	Intensity 100ppm	Intensity 25ppm	Intensity 6ppm
2	190	3929	1990	553
3	152	4533	2134	864
4	95	6066	2468	1029
7	74	6186	2754	1181
10	47	7082	3463	1445
11	42	7819	4234	1892

Table 2. Maximum emission intensity (at 460nm) for different concentrations of crosslinked C- dots.

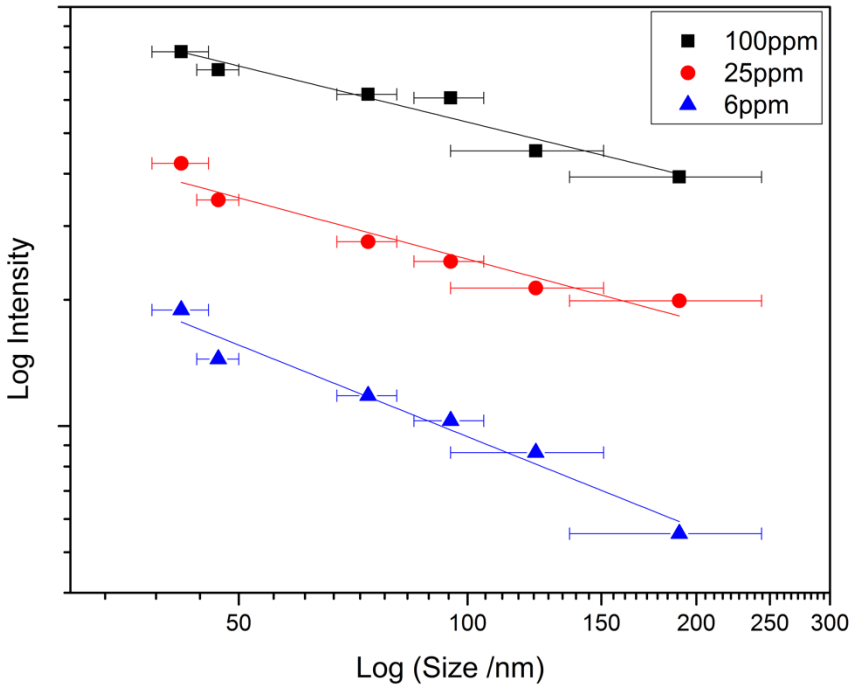

Figure 9. Maximum emission intensity vs. size of cross-linked C-dots for different solution concentration of cross-linked C-dots.

In Figure 9, different concentrations of cross-linked C-dots show the same emission property, and the three fitting lines are almost parallel. From the figure we can see that the same emission intensity is obtained for smaller particles at lower concentrations as for larger particles at higher concentrations. The crosslinked C-dot shape and PL properties are similar to the precursor C-dots. They share the same spherical morphology and they are all detectable even down to 0.4ppb. This shows the crosslinking method is an efficient way to increase the size of C-dots while preserving their PL properties.

CONCLUSION

We have developed a route to create size-controlled C-dots by crosslinking using hexamethylene diisocyanate and found the relation between the size and molar ratio of HDI to precursor C-dots that size^2 is proportion to the molar ratio. Following this rule, large size C-dots can be produced in a controlled fashion. What's more, crosslinked C-dots display the same PL properties as precursor C-dots. This suggests crosslinking we can attach C-dots on the surface of different shape particles and preserve the PL properties of the attached C-dots.

REFERENCES

(1) Li, Yan Vivian, Lawrence M. Cathles, and Lynden A. Archer. "Nanoparticle tracers in calcium carbonate porous media." Journal of Nanoparticle Research 16.8 (2014): 1-14.

(2) Michalet, X., et al. "Quantum dots for live cells, in vivo imaging, and diagnostics." science 307.5709 (2005): 538-544.

(3) Baker, Sheila N., and Gary A. Baker. "Luminescent carbon nanodots: emergent nanolights." Angewandte Chemie International Edition 49.38 (2010): 6726-6744.

(4) Li, Haitao, et al. "Carbon nanodots: synthesis, properties and applications."Journal of materials chemistry 22.46 (2012): 24230-24253.

(5) Bourlinos, Athanasios B., et al. "Photoluminescent carbogenic dots."Chemistry of Materials 20.14 (2008): 4539-4541.

(6) Tang, Chuanbing, et al. "Well-Defined Carbon Nanoparticles Prepared from Water-Soluble Shell Cross-linked Micelles that Contain Polyacrylonitrile Cores." Angewandte Chemie International Edition 43.21 (2004): 2783-2787.

(7) Xu, Xiaoyou, et al. "Electrophoretic analysis and purification of fluorescent single-walled carbon nanotube fragments." Journal of the American Chemical Society 126.40 (2004): 12736-12737.

(8) Dekaliuk, Mariia O., et al. "Fluorescent carbon nanomaterials:“quantum dots” or nanoclusters?." Physical Chemistry Chemical Physics 16.30 (2014): 16075-16084.

(9) Jia, Xiaofang, Jing Li, and Erkang Wang. "One-pot green synthesis of optically pH-sensitive carbon dots with upconversion luminescence."Nanoscale 4.18 (2012): 5572-5575.

(10) Yang, Yunhua, et al. "One-step synthesis of amino-functionalized fluorescent carbon nanoparticles by hydrothermal carbonization of chitosan." Chemical Communications 48.3 (2012): 380-382.

(11) Yang, Yunhua, et al. "One-step synthesis of amino-functionalized fluorescent carbon nanoparticles by hydrothermal carbonization of chitosan." Chemical Communications 48.3 (2012): 380-382.

(12) Hu, Sheng-Liang, et al. "One-step synthesis of fluorescent carbon nanoparticles by laser irradiation." Journal of Materials Chemistry 19.4 (2009): 484-488.

(13) Sun, Ya-Ping, et al. "Quantum-sized carbon dots for bright and colorful photoluminescence." Journal of the American Chemical Society 128.24 (2006): 7756-7757.

(14) Yang, Sheng-Tao, et al. "Carbon dots for optical imaging in vivo." Journal of the American Chemical Society 131.32 (2009): 11308-11309.

(15) Krysmann, Marta J., et al. "Formation mechanism of carbogenic nanoparticles with dual photoluminescence emission." Journal of the American Chemical Society 134.2 (2011): 747-750.

(16) Ming, Hai, et al. "Large scale electrochemical synthesis of high quality carbon nanodots and their photocatalytic property." Dalton Transactions 41.31 (2012): 9526-9531.

(17) Tian, Lei, et al. "Nanosized carbon particles from natural gas soot." Chemistry of Materials 21.13 (2009): 2803-2809.

(18) Bourlinos, Athanasios B., et al. "Surface functionalized carbogenic quantum dots." Small 4.4 (2008): 455-458.

(19) Jiang, Jie, et al. "Amino acids as the source for producing carbon nanodots: microwave assisted one-step synthesis, intrinsic photoluminescence property and intense chemiluminescence enhancement." Chemical communications48.77 (2012): 9634-9636.

(20) Zhu, Hui, et al. "Microwave synthesis of fluorescent carbon nanoparticles with electrochemiluminescence properties." Chemical Communications 34 (2009): 5118-5120.

(21) Zhu, Shoujun, et al. "Highly photoluminescent carbon dots for multicolor patterning, sensors, and bioimaging." Angewandte Chemie 125.14 (2013): 4045-4049.

(22) Liu, Ruili, et al. "An aqueous route to multicolor photoluminescent carbon dots using silica spheres as carriers." Angewandte Chemie 121.25 (2009): 4668-4671.

(23) Ray, S. C., et al. "Fluorescent carbon nanoparticles: synthesis, characterization, and bioimaging application." The Journal of Physical Chemistry C 113.43 (2009): 18546-18551.

(24) L. Tian, D. Ghosh, W. Chen, S. Pradhan, X. Chang, S. Chen, Chem. Mater. 2009, 21, 2803 – 2809.

(25) Choudhury, Snehashis, et al. "A highly reversible room-temperature lithium metal battery based on crosslinked hairy nanoparticles." Nature communications 6 (2015).

(26) Stevelmans, S., et al. "Synthesis, characterization, and guest-host properties of inverted unimolecular dendritic micelles." Journal of the American Chemical Society 118.31 (1996): 7398-7399.

(27) Woo, Seong Ihl, et al. "Polymerization of aqueous lactic acid to prepare high molecular weight poly (lactic acid) by chain-extending with hexamethylene diisocyanate." Polymer bulletin 35.4 (1995): 415-421.

(28) Damink, LHH Olde, et al. "Crosslinking of dermal sheep collagen using hexamethylene diisocyanate." Journal of Materials Science: Materials in Medicine 6.7 (1995): 429-434.

(29) Kim, C. K., B. K. Kim, and H. M. Jeong. "Aqueous dispersion of polyurethane ionomers from hexamethylene diisocyanate and trimellitic anhydride." Colloid and Polymer Science 269.9 (1991): 895-900.

(30) Caro, Salvador Ventura, C. S. Sung, and E. W. Merrill. "Reaction of hexamethylene diisocyanate with poly (vinyl alcohol) films for biomedical applications." Journal of Applied Polymer Science 20.12 (1976): 3241-3246.

(31) He, Jionghao, Kazuyuki Horie, and Rikio Yokota. "Characterization of polyimide gels crosslinked with hexamethylene diisocyanate." Polymer 41.13 (2000): 4793-4802.

(32) Krumova, M., et al. "Effect of crosslinking on the mechanical and thermal properties of poly (vinyl alcohol)." Polymer 41.26 (2000): 9265-9272.